

Semiclassical theory of elastic electron-atom scattering

Joachim Burgdörfer, Carlos O. Reinhold, James Sternberg, and Jianyi Wang*
Department of Physics and Astronomy, University of Tennessee, Knoxville, Tennessee 37996-1200
and Oak Ridge National Laboratory, Oak Ridge, Tennessee 37831-6377

(Received 14 March 1994)

We show that diffraction oscillations in elastic electron-atom scattering can be quantitatively accounted for semiclassically in terms of path interferences. The quantum scattering amplitude is expressed as a topological sum over classical and pseudoclassical paths, containing only information on the classical dynamics. The sum is shown to converge rapidly. The validity of the semiclassical theory of potential scattering is analyzed in terms of the angular-momentum dependence of the classical action for the radial motion.

PACS number(s): 34.80.Bm

Elastic differential cross sections $d\sigma/d\Omega$ for electron scattering at medium and heavy atoms display noticeable diffraction oscillations [1] with pronounced minima, which are sometimes termed “generalized Ramsauer-Townsend” (GRT) minima [2]. They play an important role not only in electron-atom scattering but also in photoelectron emission from solids [2] and electron emission in ion-atom collisions. The splitting of the binary-encounter peak [3,4], as well as peak shifts of backward emission of projectile electrons [5,6], result from GRT minima.

As is well known for some 60 years, nonrelativistic quantum theory provides a straightforward description in terms of the dominance of a very few partial waves with phase shifts δ_l in the partial-wave expression of the scattering amplitude,

$$f(\theta) = (2ki)^{-1} \sum_{l \geq 0} (2l+1)(e^{2i\delta_l} - 1)P_l(\cos\theta), \quad (1)$$

where k is the momentum of the electron and atomic units are used throughout except where otherwise stated. The minima in the cross section $d\sigma/d\Omega = |f(\theta)|^2$ are then given by the zeros (or extrema if partial-wave interference is important) of the Legendre polynomial $P_{l_0}(\theta)$ of the dominant partial wave l_0 . The fact that only a few and low angular momenta [l of the order $O(1)$] significantly contribute has led for decades to the understanding that GRT minima are a generic quantum, i.e., nonclassical effect.

Only very recently, with a resurgence of modern semiclassical methods, has renewed interest in a classical and semiclassical analysis of GRT minima arisen. The application of modern semiclassical methods to potential scattering is of considerable general interest well beyond the problem of electron-atom scattering. A large number of studies have been performed for nuclear scattering

problems [7] and, more recently, for irregular scattering in multidimensional classical nonintegrable systems [8–10].

A qualitative explanation [4] of the GRT minima in terms of semiclassical path interferences exploits the fact that the classical deflection functions for heavy atoms allow for deflection angles $\Theta < -\pi$, i.e., orbiting. Accordingly, two or more impact parameters b or angular momenta L can reach the same observation angle θ after looping around the force center. Furthermore, phase shifts δ_l can be accurately calculated semiclassically using the WKB approximation [5]. However, the further customary steps in reducing Eq. (1) to what is called the “primitive” semiclassical approximation [8], i.e., the evaluation by stationary phase approximation after converting the sum over partial waves to an integral fails [5,11]. The semiclassical path interference employing the primitive semiclassical quantization and only classical paths [11] does not reproduce the structures in the elastic electron-atom scattering cross section.

In this paper we show that GRT minima can be accurately accounted for by semiclassical mechanics if contributions beyond the primitive semiclassical approximation are properly included. Most importantly, the conventional criterion for the validity of the semiclassical approximation in terms of large angular-momentum quantum numbers, $l \gg 1$, does not need to be met.

Our analysis follows closely the seminal work by Berry and Mount [12], which appears to have found very few, if any, applications to atomic collision problems. First, the quantal phase shift δ_l is replaced by the WKB phase shift δ_L^{WKB} , which is nothing but the compensated classical action of the single-path radial motion from the turning point r_0 to infinity,

$$\delta_l \rightarrow \delta_L^{\text{WKB}} = \lim_{R \rightarrow \infty} \int_{r_0}^R k_r dr - kR + L\pi/2, \quad (2)$$

with $k_r = \{2[E - V(r)] - L^2/r^2\}^{1/2}$, and the connection between the classical angular momentum L and the l quantum number is made through the Langer correction [13] $L = l + \frac{1}{2}$. The replacement of δ_l by δ_L^{WKB} is accu-

*Present address: Physics Department, Tulane University, New Orleans, LA 70118.

rate, even for low l values over a wide range of energies for electron scattering at medium to heavy atoms [Fig. 1(a)]. This is due to the fact that the gradient of the de-Broglie wavelength $\lambda(r)$ for the radial motion, $|d\lambda(r)/dr|$, remains small over the whole range of r values, where significant deflection occurs for typical effective one-electron potentials for scattering at medium to heavy atoms. We present in the following our calculations for electron scattering at krypton. For this collision system a significant body of experimental data as well as accurate quantum calculations are available. In our calculation we use the parametrized Hartree-Fock potential of Garvey, Jackman, and Green [14]. Next, we replace the Legendre polynomials by their asymptotic expression for "large l ,"

$$P_l(\cos\theta) \cong \left[\frac{2}{\pi L \sin\theta} \right]^{1/2} \cos(L\theta - \pi/4), \quad (3)$$

which is valid for angles within the interval $1/L < \theta < \pi - 1/L$. The crucial point is that the GRT minima, which coincide with the zeros, θ_m , of P_l lie within the interval of validity, even for lowest L for which GRT minima are observed. The position of the zeros can be estimated as $\theta_m = \pi(4m+3)/4L$ (m is an integer). For angles near forward ($\theta \lesssim 1/L$) and backward directions [$(\pi - \theta) < 1/L$] alternative approximations to Legendre polynomials can be used to arrive at a semiclassical approximation for potential scattering.

Using the Poisson summation formula [15], Eq. (1) can be written as a sum over pseudopaths p ,

$$f(\theta) \approx f^{\text{SC}}(\theta) = \frac{1}{ik} (2\pi \sin\theta)^{-1/2} \sum_{p=-\infty}^{\infty} (-1)^p (e^{-i\pi/4} I_p^+ + e^{i\pi/4} I_p^-), \quad (4)$$

with

$$I_p^\pm = \int_0^\infty dL L^{1/2} \{ \exp[iS_{\text{cl}}(L, \Theta, p, \pm)] - \exp[iS_{\text{cl}}^a(L, \Theta, p, \pm)] \}. \quad (5)$$

In Eq. (5), the classical action S_{cl} is given in terms of the compensated action for the radial (S_{cl}^r) and the angular (S_{cl}^a) motion as

$$S_{\text{cl}}(L, \Theta, p, \pm) = S_{\text{cl}}^r(L) + S_{\text{cl}}^a(L, \Theta, p, \pm), \quad (6)$$

with $S_{\text{cl}}^r = 2\delta_L^{\text{WKB}}$ and $S_{\text{cl}}^a = -L\Theta$ and where the deflection angle Θ and the observation angle θ ($0 \leq \theta \leq \pi$) are related through $\Theta = \mp\theta - 2p\pi$. Note that the only approximation used so far is the WKB approximation for the phase shift [Eq. (2)] and the large- l approximation for P_l [Eq. (3)]. Equations (4)–(6) can be viewed as a semiclassical (SC) approximation to the Feynman path integral for potential scattering. It contains the topological sum over all pseudoclassical paths allowing scattering into the angle θ for all angular momenta L . The path index (p, \pm) counts the number of times a trajectory encircles the force center (nucleus) clockwise ($p > 0$) or counterclockwise ($p < 0$) and $+$ ($-$) refer to positive (negative) observation angles counted clockwise relative to the incident-beam direction (see Fig. 2). Pseudoclassical paths consist of three pieces: a classical path from ∞ to the turning point r_0 , a purely rotational motion with angular momentum L on an arc of the circle with the radius given by the turning point r_0 , and a classical path from r_0 to ∞ starting at the end point of the arc. Equation (6) gives the correct classical action for both pseudoclassical and classical paths. The intermediate segment of the path allows all L (and, hence, all impact parameters) to be scattered into a given observation angle θ and destroys the one-to-one classical relation of a single (or multi-) valued deflection function. The relative weight of pseudoclassical and true classical orbits (those with zero arc length and extremal action) is controlled by the oscillatory phase integral containing the classical action, which is the only dynamical input entering Eq. (4). One important

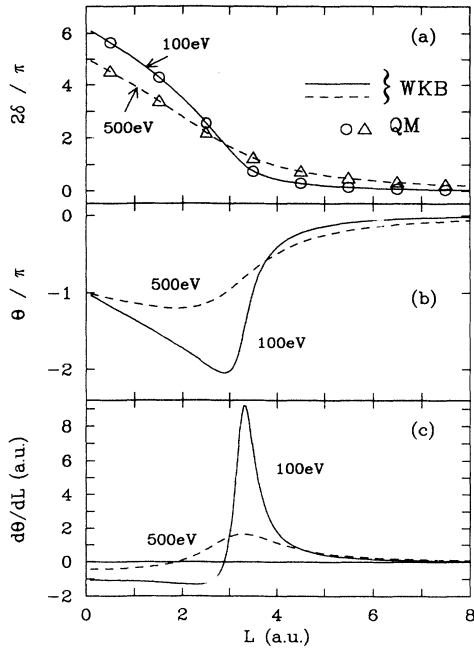


FIG. 1. Classical dynamics for electron scattering at krypton at 100 and 500 eV. (a) Quantum-mechanical (QM) and semiclassical (WKB) phase shift, (b) deflection function $\theta(L)$, and (c) second-order variation of classical action $d^2S_{\text{cl}}/dL^2 = d\theta/dL$.

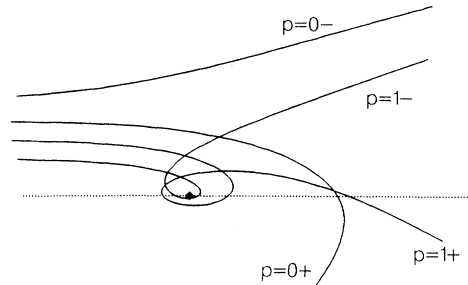


FIG. 2. Classical scattering paths with topological coding (p, \pm) relevant for generalized Ramsauer-Townsend minima.

feature of this representation is that it allows the quantitative determination of the convergence of the semiclassical approximation as a function of the number of pseudoclassical paths included and does not involve the stationary phase approximation. The role of pseudoclassical orbits has been recently also highlighted in the semiclassical theory of the spectral oscillator strength density of hydrogen in a strong magnetic field (in this context referred to as “ghost orbits” [16,17]).

If now for a given pseudoclassical path p , the classical action is sufficiently rapidly varying, the integral [Eq. (5)] can be evaluated employing the stationary phase approximation yielding the primitive semiclassical (PSC) result

$$I_{p,\text{PSC}}^{\pm} = \sum \left| \frac{2\pi L_p(\theta)}{d\Theta/dL_p} \right|^{1/2} \exp[iS_{\text{cl}}(L_p, \Theta, p, \pm) + i\alpha_p \pi/4], \quad (7)$$

where $\alpha_p = \text{sgn}(d\Theta/dL_p)$. For each path one or more stationary points may exist, yielding the corresponding branches of the classical deflection function, which is given by the stationary points of $dS_{\text{cl}}(L, \Theta, p, \pm)/dL = 0$ or, equivalently, $\theta(L_p) = 2(d\delta_L/dL)_{L=L_p}$. It is worth noting that the validity of the stationary phase approximation does not require L_p to be large. Equation (7) is valid even for $l=O(1)$ when S_{cl} varies rapidly over one unit of angular momentum, i.e.,

$$\left| \frac{d^2 S_{\text{cl}}}{dL^2} \right| = \left| \frac{d\Theta}{dL} \right| \gg 1. \quad (8)$$

This is precisely the situation we encounter near some of the GRT minima [see Figs. 1(b) and 1(c)]. The semiclassical scattering amplitude [Eq. (4)] therefore consists of a coherent superposition of contributions from pseudoclassical and true classical paths [Eq. (7)].

Electron scattering at krypton at energies of 100 and 500 eV illustrates the interplay of classical and pseudoclassical paths in semiclassical dynamics. At 500 eV the deflection function [Fig. 1(b)] features the onset of orbiting ($\Theta < -\pi$) but only one classical path for most θ . At 100 eV, on the other hand, the deflection function extends to $\Theta < -2\pi$, supplying at least two true paths for all θ . At both energies, the deflection functions contain glory and rainbow singularities. Since we employ in the analysis of GRT minima the large-angle approximation [Eq. (3)], the semiclassical corrections to glory singularities near $\theta=180^\circ$ are not included, while semiclassical rainbow scattering is treated properly. Furthermore, the criterion for the validity of the primitive semiclassical approximation [Eq. (8)] is satisfied at 100 eV over a wide range of θ , while it is only marginally satisfied over a narrow band of θ at 500 eV [Fig. 1(c)].

Figure 3 displays the rapid convergence of the topological sum over pseudoclassical paths using the classical dynamics input shown in Fig. 1. The exact sum can be approximated by just a few pseudoclassical paths with code $p=(0,+)$ and $p=(1,-)$ at $E=500$ eV and $p=(0,+)$, $p=(1,-)$, and $p=(1,+)$ at $E=100$ eV. As can be seen from Fig. 1(b), in each case only one classically forbidden

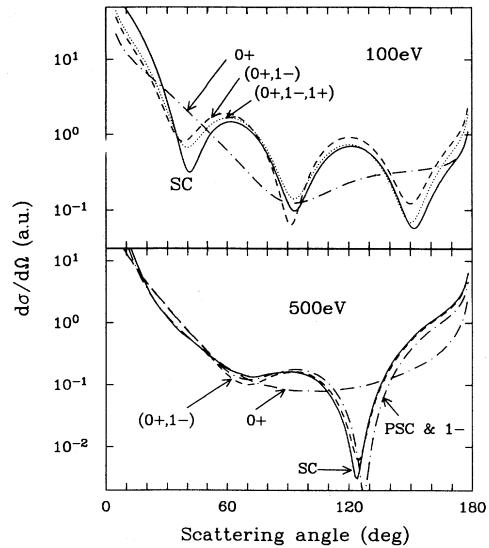


FIG. 3. Comparison of the topological partial sum for the semiclassical differential scattering cross section at 100 and 500 eV, and full Poisson sum or semiclassical (SC) results; PSC plus 1- denotes the coherent superposition of the PSC amplitude for the path (0,+) and the path-integral amplitude of path (1,-).

path [(1,+) for $E=100$ eV and (1,-) for $E=500$ eV] significantly contributes. The residual difference to the full Poisson sum is mostly due to the $p=(0,-)$ path. Furthermore, the peak in the second derivative of the classical action [Fig. 1(c)] indicates that the path integral associated with pseudopath $p=(0,+)$ for both energies possesses a stationary point, i.e., this path becomes, according to Eq. (8), classical and can be approximated by the PSC amplitude [Eq. (7)]. The resulting differential cross section (Fig. 3) containing the coherent superposition of PSC amplitudes and pseudoclassical path amplitudes (denoted by PSC plus 1- for 500 eV) approximates the exact result for the topological sum and pseudoclassical paths remarkably well.

Within the quantum description, dominance of the $l=3$ partial wave is responsible for the three GRT minima at 100 eV [$\sim |P_3(\cos\theta)|^2$]. Classical dynamics provides a simple intuitive picture: The effective electronic potential of a heavy neutral atom displays a very steep rise at its outer fringe. For example, the impact parameter for this “edge” translates at 100 eV into an angular momentum of $L \approx 3.3$. This steep rise implies several characteristic features of the classical dynamics, all of which conspire to the occurrence of generalized GRT minima: First, the classical action steeply rises with decreasing L as L approaches ≈ 3.3 [Fig. 1(a)], and second the deflection function [Fig. 1(b)] rapidly decreases from ≈ 0 to values $\Theta \lesssim -2\pi$, giving rise to orbiting and to interfering paths with the codes (0,+) and (1,-). Furthermore, the classical action shows large second-order variation [Fig. 1(c)]. Therefore, two classical paths with the codes (0,+) and (1,-) and with angular momenta close

to $l=3$ exist whose interference gives rise to the GRT minima. This provides a transparent semiclassical explanation of the dominance of a single partial wave in diffraction oscillations.

Figure 4 presents a comparison between a full nonrelativistic quantum-mechanical (QM) [Eq. (1)], the semiclassical approximation (SC) [Eq. (4)], as well as other available calculations and experimental data [18,19]. We find excellent agreement between the quantum and the semiclassical results. The remaining minor differences are not due to the usage of classical dynamics input for the scattering phase but can be traced to the "large- l " approximation to the Legendre polynomials [Eq. (3)]. However, the differences do not exceed discrepancies between different quantum calculations [20] using different effective one-electron potentials as well as relativistic corrections [21]. For completeness we also give the results for the commonly used PSC and the Airy (A) uniform semiclassical approximations using the analytic continuation into the classically forbidden region for a locally quadratic deflection function [7]. At 100 eV the PSC approximation reproduces the oscillatory pattern, which is mainly due to the interference of the $(0,+)$ and $(1,-)$ paths. However, at 500 eV, only one branch of the deflection function contributes at angles smaller than 145° and the PSC approximation fails. The path-integral representation of pseudoclassical paths is obviously far more accurate than the Airy approximation.

In summary, pronounced structures in the differential scattering cross sections referred to as generalized Ramsauer-Townsend minima provide a sensitive test for semiclassical approximations to potential scattering. We have shown that a semiclassical approximation to the path-integral representation of the scattering amplitude is accurate, even at small angular momenta and when only very few partial waves effectively contribute. Moreover, the semiclassical analysis provides an intuitive classical picture of the scattering dynamics. The semiclassical representation of the scattering amplitude as a topological sum over pseudopaths is conceptually simpler and more accurate than the uniform semiclassical approximation.

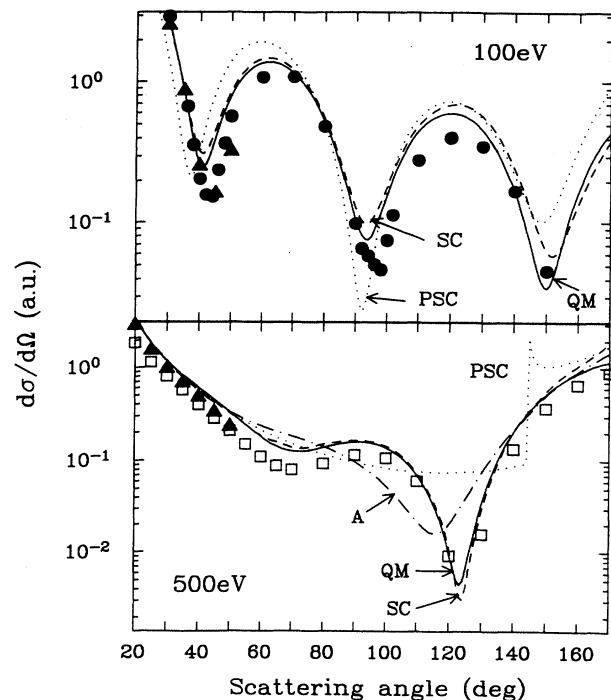


FIG. 4. Differential cross section for electron scattering at krypton at 100 and 500 eV. Present quantum-mechanical (QM), primitive semiclassical (PSC), uniform Airy (A), full semiclassical (SC, Poisson sum) results. Experimental data of Refs. [18] (\bullet), [19] (\blacktriangle), and the calculations of Ref. [20] (\square).

This work was supported in part by the National Science Foundation and by the U.S. Department of Energy, Office of Basic Energy Sciences, Division of Chemical Sciences, under Contract No. DE-AC05-84OR21400 with Martin Marietta Energy Systems, Inc. Support for one of us (J.S.) by the NSF under Grant No. PHY-9222489 is acknowledged.

[1] N. F. Mott and H. S. W. Massey, *Theory of Atomic Collisions* (Oxford University Press, New York, 1965).
 [2] See, e.g., J. J. Barton and D. A. Shirley, *Phys. Rev. B* **32**, 1892 (1985), and references therein.
 [3] C. Kelbch, S. Hagmann, S. Kelbch, R. Mann, R. E. Olson, S. Schmidt, and H. Schmidt-Böcking, *Phys. Lett. A* **139**, 304 (1989).
 [4] C. O. Reinhold, D. R. Schultz, R. E. Olson, C. Kelbch, R. Koch, and H. Schmidt-Böcking, *Phys. Rev. Lett.* **66**, 1842 (1991).
 [5] J. Wang, C. O. Reinhold, and J. Burgdörfer, *Phys. Rev. A* **44**, 7243 (1991); **45**, 4507 (1992).
 [6] M. Kuzel, R. Maier, O. Heil, D. H. Jakubassa-Amundsen, M. W. Lucas, and K. O. Groeneveld, *Phys. Rev. Lett.* **71**, 2879 (1993).

[7] D. Brink, *Semiclassical Methods for Nucleus-Nucleus Scattering* (Cambridge University Press, Cambridge, 1985).
 [8] M. Child, *Semiclassical Approximations with Molecular Applications* (Oxford University Press, London, 1991).
 [9] R. Blümel and U. Smilansky, *Phys. Rev. Lett.* **60**, 477 (1988); **64**, 241 (1990).
 [10] M. C. Gutzwiller, *Chaos in Classical and Quantum Mechanics* (Springer, New York, 1990).
 [11] W. Egelhoff, *Phys. Rev. Lett.* **71**, 2883 (1993).
 [12] M. Berry and K. E. Mount, *Rep. Prog. Phys.* **35**, 315 (1972).
 [13] R. Langer, *Phys. Rev.* **51**, 669 (1937).
 [14] R. Garvey, C. Jackman, and A. E. S. Green, *Phys. Rev. A* **12**, 1144 (1975).

- [15] P. Morse and H. Feshbach, *Methods of Theoretical Physics* (McGraw-Hill, New York, 1953).
- [16] D. Delande (private communication).
- [17] J. Delos' (private communication); J. Main, G. Wiebusch, K. Welge, J. Shaw, and J. B. Delos, *Phys. Rev. A* **49**, 847 (1994).
- [18] J. F. Williams and A. Crowe, *J. Phys. B* **8**, 2233 (1975).
- [19] R. H. Jansen and F. J. de Heer, *J. Phys. B* **9**, 213 (1976).
- [20] I. E. McCarthy, C. J. Noble, B. A. Phillips, and A. D. Turnbull, *Phys. Rev. A* **15**, 2173 (1977).
- [21] D. Walker, *Adv. Phys.* **20**, 257 (1971); K. Hasenburger, D. H. Madison, K. Bartschat, and K. Blum, *J. Phys. B* **19**, 1803 (1986).